AD-A154 877 FINITE ELEMENT METHODS FOR VISCOELASTIC FLOW(U) 1/1
WISCONSIN UNIV-MADISON MATHEMATICS RESEARCH CENTER
D S MALKUS APR 85 MRC-TSR-2812 DAAG29-80-C-0041
UNCLASSIFIED F/G 20/4 NL

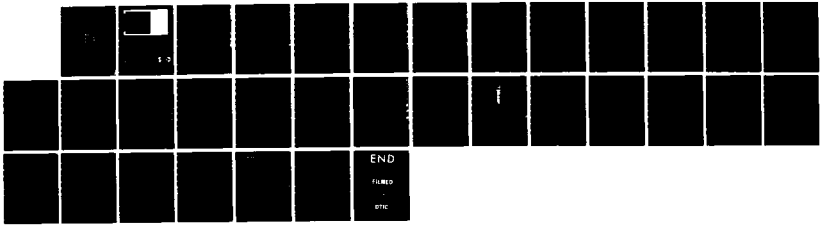

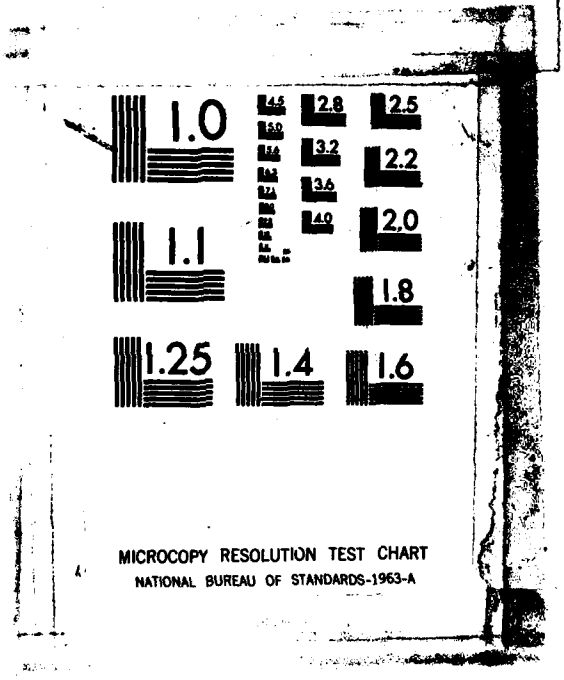
1.0
1.1
1.25
1.4
1.6
1.8
2.0
2.2
2.5
2.8
3.2
3.6
4.0
4.5
5.0
MICROCOPY RESOLUTION TEST CHART
NATIONAL BUREAU OF STANDARDS-1963-A

(2)

AD-A154 877

MRC Technical Summary Report #2812

FINITE ELEMENT METHODS FOR VISCOELASTIC FLOW

David S. Malkus

Mathematics Research Center
University of Wisconsin—Madison
610 Walnut Street
Madison, Wisconsin 53705

April 1985

(Received April 11, 1985)

DTIC FILE COPY

DTIC ELECTE JUN 11 1985 S D G

Sponsored by

U. S. Army Research Office
P. O. Box 12211
Research Triangle Park
North Carolina 27709

Air Force Office of
Scientific Research
Washington, DC 20332

National Science Foundation
Washington, DC 20550

85 06 10 164

UNIVERSITY OF WISCONSIN-MADISON
MATHEMATICS RESEARCH CENTER

FINITE ELEMENT METHODS FOR VISCOELASTIC FLOW

David S. Malkus*

Technical Summary Report #2812
April 1985

ABSTRACT

Finite element methods to compute approximate solutions to flow problems involving the flows of viscoelastic fluids are discussed. The primary goals of such investigations are at least three: First, to evaluate the predictions of the many proposed constitutive theories for viscoelastic fluids. Second, to model measurement flows in various rheological measurement devices in order to quantify the deviation of the actual flow from the flow which must be presumed to interpret the measurement. Third, it is hoped that these methods will prove sufficiently robust to allow the simulation of idealized polymer processes with the aim of aiding in the design of such processes and the required apparatus. The focus of the current research of the author and a growing number of others is on two-dimensional, isothermal, steady flows of incompressible fluids. While these restrictions will be seen to be non-essential in theory, even the simplest calculations of non-viscometric flow solutions will be seen to require a high degree of computational complexity in practice. Nevertheless, the current finite element procedures seem to show promise in the continuing endeavor to understand this challenging class of problems.

AMS (MOS) Subject Classifications: 65N30, 76A05, 76A10

Key Words: constitutive equation, viscoelastic fluid, finite element, measurement flow, differential model, integral model, characteristics, streamlines, hole-pressure.

Work Unit Numbers 2 and 3 (Physical Mathematics; Numerical Analysis and Scientific Computing)

* Sponsored by the United States Army under Contract No. DAAG29-80-C-0041, the United States Air Force under Grant No. 84-NM-399 and the National Science Foundation under Grant Nos. MCS 79-03542, 81-02089 and 83-01433.

FINITE ELEMENT METHODS FOR VISCOELASTIC FLOW

David S. Malkus*

INTRODUCTION

The idea to apply finite element methods to viscoelastic fluid flow problems, as opposed to finite difference methods, seems to have stemmed from the desire to model a variety of industrial polymer processes, which were often characterized by complex flow geometries. In the early work of Tanner, Nickel, and Bilger [1], one gets the clear idea that the hope was to develop a rather general-purpose code which could be used by the industrial rheologist to tackle geometrically complicated flow situations, particularly those flows like the extrusion of a jet of liquid material, in which the complex geometry itself was unknown a priori. Finite elements seem to be ideal tools for such modelling because of their geometric flexibility. Since ref. 1 appeared, it has been discovered that there were a number of unanswered questions about the modelling of viscoelastic fluids, which are even more basic than the choice of discretization scheme. Many of the problems currently being solved by this author and others are of an idealized nature and involve little geometric complexity, so that they could just as easily be attacked by finite differences, and the questions to which we seek answers could as well be asked about difference methods or element methods. There are a number of investigators who have, in good fluid-mechanical tradition, opted for finite difference methods [2-4]. Much of what is said here could equally apply to the difference approach, but in order to limit the present discussion to the manageable, only finite element methods will be discussed here.

The reader should be forewarned that the author's own predilection is for the development of general purpose methods which can be applied to broad classes of viscoelastic fluid flow problems in complex geometries without reprogramming. His hope is that once the basic difficulties involving choice of constitutive equation, convergence of nonlinear iteration methods. the effect of singularities of unkown order — and others still — are more firmly in hand, the vision on ref. 1 may be more completely realized. In the meantime, the author and other researchers have tended to solve problems which do not tax the geometric flexibility of the finite element formulation (and consequentially, do not illustrate

* Sponsored by the United States Army under Contract No. DAAG29-80-C-0041, the United States Air Force under Grant No. 84-NM-399 and the National Science Foundation under Grant Nos. MCS 79-03542, 81-02089 and 83-01433.

its power). These are flows which might be classified as "measurement flows" in many cases — very well-characterized flows which can be established in laboratory situations for the purposes of making measurements of material properties. The lack of geometric complexity leads to flows which can be idealized as flows for which the equations of motion can be solved analytically; however, the real flow is some perturbation of the idealized flow: Cone-and-plate [5] flow actually has free surfaces, though it is observed that this does not lead to an unacceptable disturbance in the assumed form of the flow-field, at low enough shear-rate. The entrance into a slit-die [5] perturbs the flow-field in the entry region, but the velocity field and pressure gradient soon readjust themselves to those characteristic of channel flow, at least at low enough shear-rate. There are many other such flows, including plane flow over a transverse slot, discussed below. The common characteristic of such flows is that they are perturbations of known flows; we know rather well what qualitative features the numerical results must display. On the other hand, the effect the perturbation of the assumed flow may have on the measurements, particularly at the extreme range of shear-rate, is a question which seems to be appropriately addressed by numerical modelling. So such flows seem to be modest testing grounds for the methods under discussion here, yet also seem to raise questions to which numerical modelling may be able to supply useful answers.

We will see that investigations of such problems, humble though they be compared to what might be envisaged, raise thorny questions which are still only partially resolved. The questions seem to have at their heart the question of what constitutive equation should be used and why. The choice of constitutive equation will be seen to govern a basic decision about the kind of finite element method which must be used. It will be observed that different constitutive equations can lead to radically different behavior of the numerical method, yet there seems to be little to differentiate between them on physical grounds.

CONSTITUTIVE EQUATIONS

Perhaps the most basic choice in the design of a numerical method devolves from the fact that there are two seemingly different classes of constitutive equations which have been proposed by rheologists and which seem to be numerically tractable: the *differential* and the *integral* [6-9]. What is meant specifically by these terms will be defined shortly; the important thing to note is that these are intersecting classes of constitutive equations, yet neither class seems to entirely contain the other. At first sight, the two classes of

constitutive equations seem to demand totally different numerical methods, forcing the numerical modeller to make an irrevocable choice of methodology at the outset. An important point to be observed here is that there is more in common between the two classes of equations than first meets the eye, and thus the potential exists for a more unified numerical approach than is the current practice.

General Differential Constitutive Equation

$$\begin{aligned} \boldsymbol{\sigma} &= -p\mathbf{I} + 2\mu(0)R\dot{\mathbf{e}} + (1-R)\boldsymbol{\Sigma} \\ \boldsymbol{\Sigma} &= \sum_{k=1}^{N} \boldsymbol{\tau}_k \end{aligned} \tag{1}$$

where $\mu(0)$ is the zero-shear viscosity, $\dot{\mathbf{e}}$ the strain-rate tensor, $R < 1$ is a retardation ratio defined by $R = \Lambda/T$ for a characteristic relaxation time, T, and retardation time, $\Lambda < T$, and p is the hydrostatic pressure function. The terms on the right-hand side of eq. (1) may be interpreted as an isotropic contribution to the stress, the Newtonian contribution to the stress — possibly arising from a Newtonian solvent — and the viscoelastic contribution to the stress, respectively.

The "extra stress" tensor, $\boldsymbol{\Sigma}$, determines the non-Newtonian contribution to the total stress tensor. In a differential constitutive equation, it is determined by one auxiliary equation for each of the "partial stresses," $\boldsymbol{\tau}_k$ [8],

$$\begin{aligned} \lambda_k \frac{\Delta \boldsymbol{\tau}_k}{\Delta t} + \mathbf{B_k} &= \mathbf{0} \\ \frac{\Delta \boldsymbol{\tau}}{\Delta t} &\equiv \frac{\partial \boldsymbol{\tau}}{\partial t} + (\mathbf{v}\cdot\nabla)\boldsymbol{\tau} - \boldsymbol{\tau}(\nabla\mathbf{v})^T - (\nabla\mathbf{v})\boldsymbol{\tau} \end{aligned} \tag{2}$$

where λ_k is the k^{th} relaxation time in a relaxation spectrum (which may be infinite). The T mentioned above can be taken to be a mean relaxation time in the spectrum. $\mathbf{B_k}$ is a tensor function which may depend on velocity gradients and stresses(in a possibly nonlinear fashion). Specific examples will be cited below. Note that the upper convected time derivative, $\frac{\Delta \boldsymbol{\tau}}{\Delta t}$, has unknown stresses multiplying unknown velocity derivatives, and problems with such constitutive equations are inherently nonlinear, even for the simplest linear choices of $\mathbf{B_k}$. With the obvious correspondence of notations, eqs. (1) and (2) are in the same form as the corresponding equations in ref. 6, generalized slightly in order to allow the possibility of more than one partial stress.

General Single-Integral Constitutive Equation

The single-integral designation is intended to make a distinction between the constitutive equations under consideration here and those involving multiple, iterated integrals. In fact, the theories described here may involve sums of more than one "single integral." While it makes perfect sense to consider transient flows with single-integral constitutive equations, the computational complexity implied by such flows is such that a new generation of bigger, faster computers would probably be required. Here we consider steady flows only, whereas no such restriction was imposed on our discussion of differential constitutive equations. The assumed general form of the stress field is given by

$$\boldsymbol{\sigma} = -p\mathbf{I} + 2\mu(0)R\dot{\mathbf{e}} + (1 - R)\boldsymbol{\sigma}' \tag{3}$$

where the symbols in the first two terms are the same as those in eq. (1). The extra stress in eq. (3) is given by $\boldsymbol{\sigma}'$, which plays an analogous role to $\boldsymbol{\Sigma}$ in eq. (1). For the integral constitutive equations, however, the extra stress is given by an explicit calculating formula, rather than implicitly, as in eq. (1). It is assumed to have the form

$$\boldsymbol{\sigma}' = \sum_{l=1}^{M} \int_{-\infty}^{0} \mathbf{S}_0{}^{(l)}(\tau) m_l(\tau)\, d\tau \tag{4}$$

where m_l is a memory function, and $\mathbf{S}_0{}^{(l)}$ is a strain-measure. The memory function $m_l(\tau)$ has the following form in most examples of which we are aware:

$$m_l(\tau) = T^{-1} \sum_{k=1}^{N_l} G_k^{(l)} p_k^{(l)} exp(\frac{\tau p_k^{(l)}}{T}) \tag{5}$$

The constants $G_k^{(l)}$ and $p_k^{(l)}$ whether chosen experimentally or theoretically, must be chosen so that $\int_{-\infty}^{0} q(\tau) m_l(\tau)\, d\tau < \infty$, for all polynomials, q, of arbitrary degree. This is automatic unless $N_l = \infty$, which does occur in practice. In fact, one can see that by interchanging the order of integration in eq. (4) with the summation in eq. (5), the stress contribution of each of the single integrals in eq. (4) becomes a sum of partial stresses, each associated with a member of the relaxation spectrum, T/p_k, each given by integration of a strain-measure against a single exponential. Thus T/p_k in eq. (4) and λ_k in eq. (2) are analogous relaxtion times, and $\boldsymbol{\Sigma}$ and $\boldsymbol{\sigma}'$ are analogously expressed as sums of partial stresses.

For some differential constitutive equations, the relation between them and a rearrangement of eq. (4) into partial stress form is more than an analogy; the integral

constitutive equation amounts to a direct solution of the hyperbolic equations (2) for a fixed velocity field along the streamlines, which turn out to be a double family of real characteristics [11]. Examples of this will be pointed out subsequently. It is important to note that this correspondence between integral and differential constitutive equations only holds in very special cases. There are constitutive equations derived on physical grounds, which have an integral form, yet cannot be identified as characteristic solutions of any differential constitutive equation given by eq. (2). Likewise, there are differential constitutive equations which do not seem to yield to closed-form solutions along the characteristics in the form of eq. (4).

The strain measures in eq. (4) are assumed to have the following dependencies:

$$\mathbf{S_0}^{(l)} = \mathbf{S_0}^{(l)}(\mathbf{E_0}(\tau), \mathbf{E_0}^{-1}(\tau), \nabla \mathbf{v}|\mathbf{x}(\tau)|, \nabla \mathbf{v}|\mathbf{x}(0)|) \tag{6}$$

$\mathbf{x}(0)$ is the position at which $\boldsymbol{\sigma}'$ is evaluated in the current configuration of the fluid. $\mathbf{x}(\tau)$ is that particle's position at time τ in the past, and $\mathbf{v}$ is the velocity field carrying $\mathbf{x}(\tau)$ to $\mathbf{x}(0)$, inducing the stress field. $\mathbf{E_0}(\tau)$ is a deformation-gradient measuring the strain in the deformation at time τ relative to time 0, induced by $\mathbf{v}$. $\mathbf{E_0}(\tau)$ may be the usual $\frac{\partial \mathbf{x}(\tau)}{\partial \mathbf{x}(0)}$ or something similar but somewhat different. It can be chosen to correspond to various convected derivatives in differential models [8,9] and can physically represent the strain due to molecules which undergo motion relative to the motion of the continuum (non-affine motion) [9,12].

To compute the deformation-gradient, it is neccessary to construct the path $\mathbf{x}(\tau)$, which is a streamline; the gradient is a measure of strain at the historical time and position along that path and the present position. The following equations describe the path and strain:

$$\begin{aligned} \dot{\mathbf{x}}(\tau) &= \mathbf{v}|\mathbf{x}(\tau)| \\ \mathbf{x}(0) &= \mathbf{x_0} \\ \dot{\mathbf{E}}_0(\tau) &= \mathbf{F}(\mathbf{x}(\tau); \nabla \mathbf{v}|\mathbf{x}(\tau)|)\mathbf{E_0}(\tau) \\ \mathbf{E_0}(0) &= \mathbf{I} \end{aligned} \tag{7}$$

where $tr\mathbf{F} = 0$ for all $\tau < 0$. Note that this is a system of equations to be solved in reverse time. The first group is possibly nonlinear and determines the streamline; the second group is a linear system whose non-constant coefficient is determined by the streamline solution. It is also not hard to deduce that $\mathbf{E_0}(\tau)$ is the identity in the present configuration and maintains $det(\mathbf{E_0}(\tau)) = 1$ for all historical time [10].

Examples:

1. Differential only:

   (a) Phan-Tien/Tanner (PTT) [6]

$$N = 1,\ T = \lambda,\ \eta = (1 - R)\mu(0)$$

$$\mathbf{B} = \mathbf{B}_1 = \tau exp\{\frac{\lambda\epsilon}{\eta} tr\tau\} - 2\eta\dot{\mathbf{e}} + \lambda\xi(\dot{\mathbf{e}}\tau + \tau\dot{\mathbf{e}})$$

   ξ is a non-dimensional parameter of the model, as is ϵ; When the latter parameter is not zero, there is no known integral form of the PTT equation.

   (b) Leonov [6], White-Metzner, etc. [7].

2. Integral only:

   (a) Doi-Edwards [13]

$$M = 1,\quad N = \infty,\quad p_k = (2k-1)^2$$

$$G_k = C/Tp_k,\quad \mathbf{F} = \nabla\mathbf{v},\ C = \frac{96\mu(0)}{\pi^4}$$

$$\mathbf{S_0}(\tau) = \phi_1(I, II)\mathbf{C_0^{-1}}(\tau) + \phi_2(I, II)\mathbf{C_0}(\tau)$$

$$\mathbf{C_0}(\tau) = \mathbf{E_0}^T(\tau)\mathbf{E_0}(\tau)$$

   The scalar functions ϕ_1 and ϕ_2 are functions of the two nontrivial principal invariants, I and II, of $\mathbf{C_0^{-1}}(\tau)$.

   (b) Curtiss-Bird [14]

$$M = 2,\ N_1 = N_2 = \infty,\ p_k^{(1)} = p_k^{(2)} = p_k = (2k-1)^2$$

$$G_k^{(1)} = C_1/Tp_k,\ G_k^{(2)} = C_2/p_k^2,\ \mathbf{F} = \nabla\mathbf{v}$$

$$C_1 = \frac{96\mu(0)}{\pi^4(1 + 2\epsilon/3)},\ C_2 = \frac{\epsilon 192\mu(0)}{\pi^2(1 + 2\epsilon/3)}$$

   $\mathbf{S_0}^{(1)}$ is the same as $\mathbf{S_0}$ of (2a), and $\mathbf{S_0}^{(2)}$ is a more complicated tensor function of $\mathbf{C_0}$, $\mathbf{C_0^{-1}}$, and $\nabla\mathbf{v}(0)$ [10,14]. ϵ is the "link-tension" coefficient, a non-dimensional parameter of the model; with $\epsilon = 0$, the Curtiss-Bird equation reduces to the Doi-Edwards.

3. Both differential and integral:

   (a) Oldroyd/Jeffreys (taking $N = 1$ for simplicity. not necessity) [8,9]

$$T = \lambda,\ N = 1$$

$$\mathbf{B} = \tau - 2(1 - R)\mu(0)\dot{\mathbf{e}} + \lambda a(\dot{\mathbf{e}}\tau + \tau\dot{\mathbf{e}})$$

Note that taking $\xi = a$ and $\epsilon = 0$ in (1a) yields (3a).

(b) Johnson-Segalman (with a nonzero R) [9,12]

$$T = \lambda, \quad N = M = 1, \quad p_1 = 1$$

$$G_1 = \mu(0)/\lambda, \quad \mathbf{F} = a\dot{\mathbf{e}} - \dot{\boldsymbol{\omega}}$$

$$\mathbf{S}_0(\tau) = \mathbf{E}_0^{-1}(\tau)\mathbf{E}_0^{-\mathbf{T}}(\tau) - \mathbf{I}$$

A-1

(3b) is the integral form of (3a) (and thus of a special case of (1a)) [9]. $\dot{\boldsymbol{\omega}}$ is the vorticity tensor. The parameter a is a "slip parameter" in the derivation of (3a), which allows for non-affine motion of a strained molecular lattice with respect to the continuum [9,12].

CHARACTERISTICS AND NUMERICAL METHODS

Steady Plane Flow of a Johnson-Segalman Fluid

The author has performed computations with the fluid described by (3a) and (3b). Since his computations employ the integral form of the constitutive equation, he refers to the model as Johnson-Segalman. It turns out that, for the purposes of analyzing the system of equations to be solved, it is easier to deal with the differential form (3b). The analysis discussed here has only been carried out for this one differential constitutive equation (it does include several simple Maxwell - type equations for particular choices of a [9]). It is hoped that the conclusions hold for other differential models — and because of the analogy alluded to earlier — to integral models as well. In what follows, take $R = 0$ and $N = 1$.

The assumed form of the equations of steady motion is

$$\nabla \cdot \boldsymbol{\sigma} + \mathbf{f} = \rho(\mathbf{u} \cdot \nabla)\mathbf{u} \tag{8}$$

where $\mathbf{u}$ is the (two-dimensional) velocity field, $\boldsymbol{\sigma}$ is the stress field, $\mathbf{f}$ a body force, and ρ the fluid density. At present it is assumed that the flow is a plane flow, and that the material is exactly incompressible,

$$\nabla \cdot \mathbf{u} = 0 \tag{9}$$

For the Johnson-Segalman fluid with parameters as specified, the equations of stress, mo-

tion, and continuity take the form

$$\begin{aligned} &\lambda\frac{\Delta\tau}{\Delta t} + \mathbf{B} = \mathbf{0} \\ &\rho(\mathbf{u}\cdot\nabla)\mathbf{u} + \nabla p - \nabla\cdot\tau = \mathbf{0} \\ &\nabla\cdot\mathbf{u} = 0 \end{aligned} \tag{10}$$

The analysis of ref. 11 begins by observing that in this differential form, eqs. (10) are a quasilinear system, whose characteristics may be given explicitly in terms of a solution. The analysis of ref. 13 reveals that *below a critical stress*

I. For a fixed $\mathbf{u}$, the stress equations are *hyperbolic*.

II. Streamlines are a double family of real characteristics of the stress equations.

III. Solution for τ by the method of characteristics yields a problem which is *elliptic* in $\mathbf{u}$. The stress is given by an integral stress calculator of the form of eq. (4).

It should be noted that the sense in which the equations of motion are elliptic must be carefully qualified: There are no real characteristics of the equations of motion alone, below the "sonic transition" (critical stress). But since there may be characteristics entering through boundaries at inflows (with corresponding outflows), stress data — or the equivalent — must be somehow specified there. So the whole problem is not elliptic in the usual sense, when characteristics cross domain boundaries.

There is a way to make the equations of motion elliptic in the usual sense when a given stress field is specified, and that is to rewrite eq. (10) in equivalent form,

$$\begin{aligned} &\lambda\frac{\Delta\tau}{\Delta t} + \mathbf{B} = \mathbf{0} \\ &\rho(\mathbf{u}\cdot\nabla)\mathbf{u} + \nabla p - \mu\nabla^2\mathbf{u} = \nabla\cdot\tau - \mu\nabla^2\mathbf{u} \\ &\nabla\cdot\mathbf{u} = 0 \end{aligned} \tag{10a}$$

in which μ is a positive, viscosity-like constant. In an iterative solution method which uses the right-hand side of the middle equations of eqs. (10a) from a previous velocity iterate and the stresses calculated from the hyperbolic stress equations in that velocity field, solution for the next velocity iterate can be a truly elliptic problem. This is exploited in some of the methods to which we now turn our attention.

The Spectrum of Discrete Methods

The results of ref. 11 have interesting ramifications for numerical methods for viscoelastic fluids. In what follows, we assume that computations are to be carried out in a steady flow regime below the critical stress for type-change (numerical experiments by the author suggest that with the contitutive equations currently employed, the critical stress is so large as to be essentially inaccessible by current numerical methods). We assume that the characteristics of the equations to be solved for any constitutive equation of the forms considered in this paper are the same as they are in the Johnson-Segalman case. While the analysis has not been carried out in such generality, this assumption does not seem unwarrented in the light of numerical evidence. The methods currently employed by most researchers fall somewhere on the spectrum of methods given in Table 1.

METHOD	MIXED	STRESS ALT. $\mathbf{v}, p$		PURE $\mathbf{v}, p$	
KEY FEATURE	All at once	Variant 1 Total numerical	Variant 2 Meth. chars.	Numerical Streamline	Analytic Streamline
PDE TYPE	Mixed	Hyperbolic/Elliptic	Hyperbolic/Elliptic	Elliptic	Elliptic
UNKS.	$\mathbf{u}, \tau, p$	τ $\mathbf{u}, p$	τ $\mathbf{u}, p$	$\mathbf{u}, p$	$\mathbf{u}$
REFS.	[7],[15], [16],[17]	[18]	[18]	[7], [19], [20]	[7], [10]

Table 1

Spectrum of Finite Element Methods for Viscoelastic Flow.

t the extreme left end, there is a class of methods applicable, in principle, to any consti-
itive equation which has a differential form. These methods treat the quasilinear system
a system of mixed type and discretize velocity, pressure, and extra stress independently
a mixed/Galerkin method. At the extreme right end of the spectrum are methods which
pply to those constitutive equations which have an integral form. They discretize only
ial velocity fields in an iterative sequence of approximations to the solution of the equa-
ons of motion and continuity; even the pressure can be eliminated if a penalty approach is
ed. In these right-wing methods, stress is computed via the integral stress calculator of
q. (4) as a functional of the trial velocity fields. Each of the extreme right- and left-wing
ethods have their own distinct advantages and disadvantages. Left-wing, mixed methods
ed many stress unknowns — particularly if more than one relaxation time and corre-
onding partial stress must be discretized. Left-wing methods thus involve large matrices
ith large bandwidths, but transient problems can be solved by well-known time-stepping
ethods. Left-wing methods also require the specification of boundary data where charac-
ristics emanate from boundaries. How to specify such data for partial stresses is a subtle
atter [11], and the possiblity of over or under specifying boundary data is real one. On
e other hand, left-wing methods give the Galerkin residual in terms of stress unknowns,
hich are primary variables; thus differentiation of the Galerkin residuals with respect to
odal variables as required to form Newton's method for solving the discrete nonlinear
alerkin equations is straight-forward.

The right-wing methods make some direct trades of advantage for disadvantage when
mpared to the left-wing methods. Only velocities need be discretized; computational
ork is not increased by adding more relaxation times. The specification of stress on
coming characteristics can be handled implicitly, in a way that seems to work rather
ell, if not theoretically justified at present. The incoming streamlines are assumed to be
ose of a known flow extending to infinity in a known geometry (such as channel flow), and
us the required contributions to the integrand of eqs. (4) and (11) are actually known
alytically once the particle enters this "predecessor flow" [10,19]. On the other hand,
ansient methods seem nearly impossible, and Newton's method seems difficult, at best,
cause of the complicated functional relation between the stresses in the Galerkin residual
d the velocity field. In most cases, it seems that the choice of left-wing and right-wing
ethod is made a-prio by the form of the constitutive equation: integral models seem to
mand right-wing methods and differential left-wing methods.

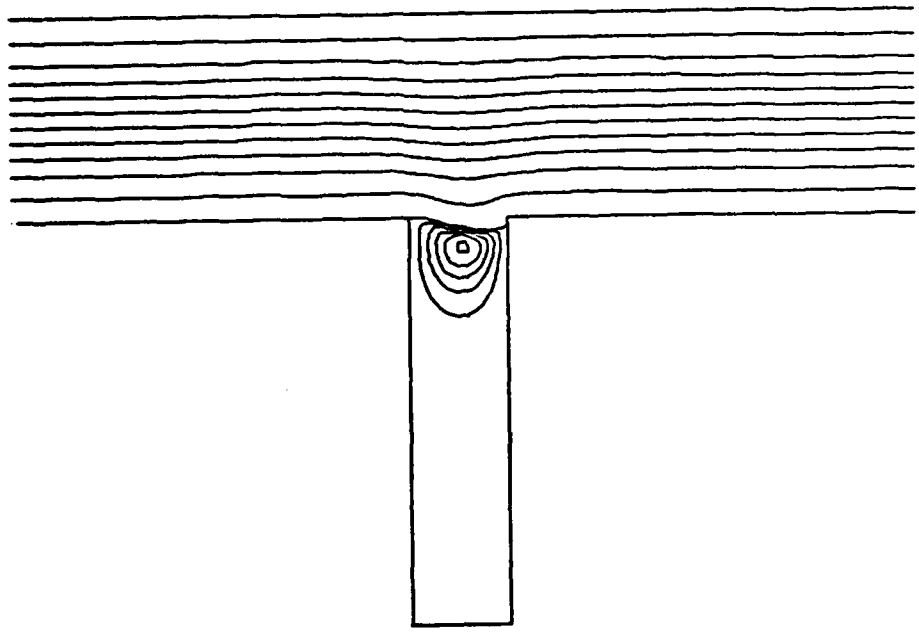

Figure 7

Flow with the Concocted Constitutive Equation at $D_e = 3.7$.

The flow pictured in Figure 6 has $D_e = 2.5$, $L_o = 1.8$, and viscosity reduced to 46% of its zero-shear value. The flow of Figure 7 is at $D_e = 3.7$, but $L_0 = 1.6$, which is lower than the stress-ratio of Figure 6; in Figure 7, the viscosity is 40% of its zero-shear value. The stress-ratio of the concocted fluid model goes through a maximum, due to the retardation time; the flow of Figure 6 has shear-flow at the wall which is just about at that maximium. 16 Laguerre integration points were used for the quadrature of eq. (11) when computing the flows of Figures 6 and 7.

In both the flows of Figure 6 and Figure 7, the Broyden iteration scheme had a tougher time converging than it did with the Curtiss-Bird fluid at a much higher D_e and L_o. The $D_e = 3.7$ case took 40 iterations to get only a factor of 25 reduction in the residual. Attempts to converge at higher D_e failed. The $D_e = 2.5$ case took 20 iterations to get a factor of 20 reduction in the residual. Thereare some qualitative differences between the flows of Figures 6 and 7 and the flow of Figure 5. These may be related to the greater difficulty in convergence, though this cannot be stated with any certainty. We note that the streamlines just outside the slot are, if anything, more distorted by the presence of the

damping function

$$\phi(II) = exp(-c\sqrt{II - 3}) \tag{22}$$

which just multiplies the strain-measure, $\mathbf{S_0}$, of the Johnson-Segalman model. II is the second principal invariant of the *non-affine* strain measure, $\mathbf{E_0^{-1}E_0^{-T}}$ No physical reasoning lies behind this; damping functions are intended to account for the effect of breaking temporary junctions in the lattice under large strain. To what extent this would happen if non-affine motion of the lattice is allowed, or, if so, whether the damping function for a non-affine strain-measure should take the form of eq. (24) is unknown. At any rate, the flow of Figures 6 and 7 use this concocted model, and take $c = 0.1$; the other parameters were as just described for the Johnson-Segalman with a retardation time.

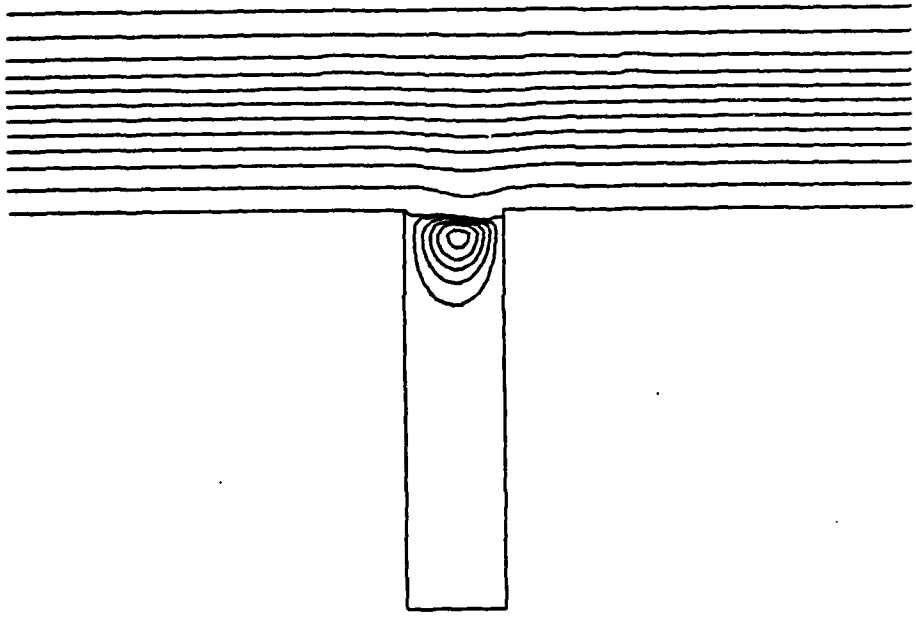

Figure 6

Flow with the Concocted Constitutive Equation at $D_e = 2.5$.

constitutive equations [2,7,16,20]. The run was terminated when the residual measure of ref. 10 had been reduced by a factor of 84 (a similar reduction factor to those reported in ref. 10). The residual appeared to be continuing to converge, but the computation was terminated because the experience of ref. 10 shows that most quantities of interest have stabilized to a couple of decimal digits with a comparable residual reduction. This residual reduction was accomplished in 18 inverse Broyden iterations. The computation took 15 hours of VAX 11/780 CPU time on a VAX with a standard configuration, using double precision hardware.

There are several interesting features of Figure 5. The flow is from right to left, and we observe substantial vortex distortion of the type observed in ref. 4. We also note that there is little disturbance in the streamlines near the mouth of the slot when compared to those in the Stokes-flow of Figure 4 or the streamlines in the flow visualizations of ref. 4. Also, of the five equally-spaced streamlines in the slot, three are crowded together near the dividing streamline; this indicates that the velocity of fluid in the vortex is lower compared to the velocity at the dividing streamline in the non-Newtonian case than it is in Stokes-flow. This appears to be due to shear-thinning; the viscosity in undisturbed flow at the wall in the case of Figure 5 is only 9% of its zero-shear value. The very high driving stresses in the die are not transmitted to the slot, and the fluid slides by without feeling much effect of the slot.

We turn our attention to the flow of another fluid in the same geometry, using the same mesh as before. The author really would have liked to have shown results involving a Johnson-Segalman fluid at significant D_e, but these are not available. Johnson and Segalman found that a value of their slip-parameter of $a = 0.87$ gave good agreement of viscometric functions with published data [12]. With this value of a, a very high zero shear viscosity (implying negligible Reynolds number), and $R = 0$ in eq. (3), the inverse Broyden iterations of eq. (18) diverge dramatically at about $D_e = 1.0$. Adding a substantial Newtonian viscosity with $R = 1/3$ helps some, as one might expect, but divergence ensues at a disappointing $D_e = 1.5$. In order to obtain an integral constitutive equation which shear thins less than Curtiss-Bird, behaves better than Maxwell, does not imply *very* peculiar lattice motion which would be the result of taking a very small slip-parameter [9], and which allows computation with at least a moderate D_e. the author just tinkered with the Johnson-Segalman equation. Favorable results were obtained by adding a Wagner-type

D_e is the "Deborah number" and L_o the "stress-ratio." $\dot{\gamma}$ is the shear-rate at the wall of the die, far from the slot, and N_1 and σ are taken at the same location. For the flow pictured in Figure 5, $D_e = 17.9$, and $L_o = 4.1$; the computation used the Curtiss-Bird equation [10,14], with the same parameters given in ref. 10 for the "EFN Fluid." This is intended to model a high-viscosity, concentrated polymer system without significant branching of the molecular chains. The resulting viscosity is so high ($\approx 10^4$ poise at zero shear) that the Reynolds number is negligible, even when shear-thinning is accounted for.

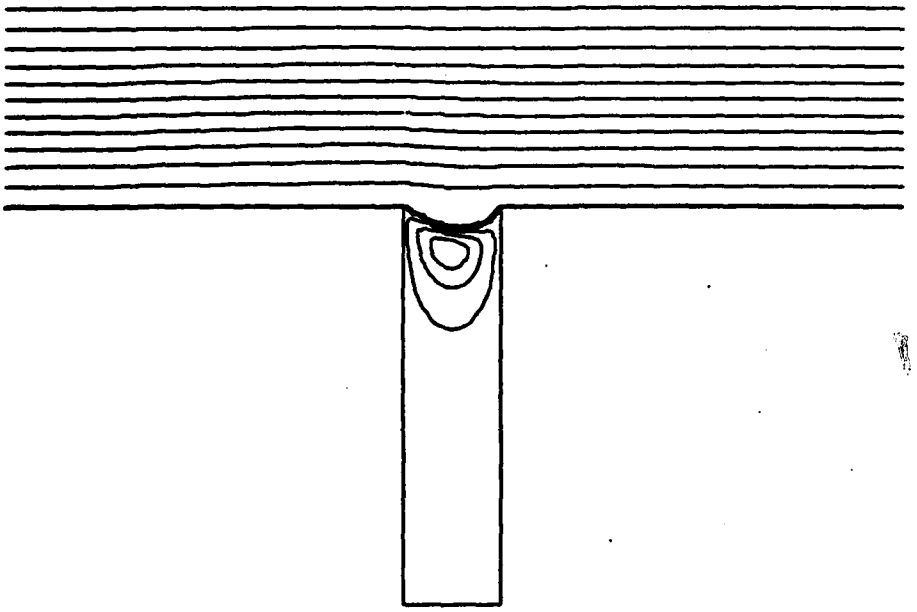

Figure 5
Flow of a Curtiss-Bird Fluid at $D_e = 17.9$.

The computations of ref. 10 were carried out with Gaussian memory formulas (eq. (11)) with ten points; computations were reported there up to $D_e = 7.5$. It has since been determined that the ten-point Gaussian formula loses its accuracy in simple shearing flow (and thus in the undisturbed die-flow) for D_e much larger than that. Furthermore, one observes that the ten-point formula is inaccurate enough to lead to an artificial shear-stress maximum [10,20] for very high D_e. For that reason, the computations leading to Figure 5 were carried out with 18-point formulas for each memory-integral. With the 18-point formula, no difficulty in convergence of the Broyden iterations was observed — no "barrier" or "high Weissenberg number problem" which has been observed for other

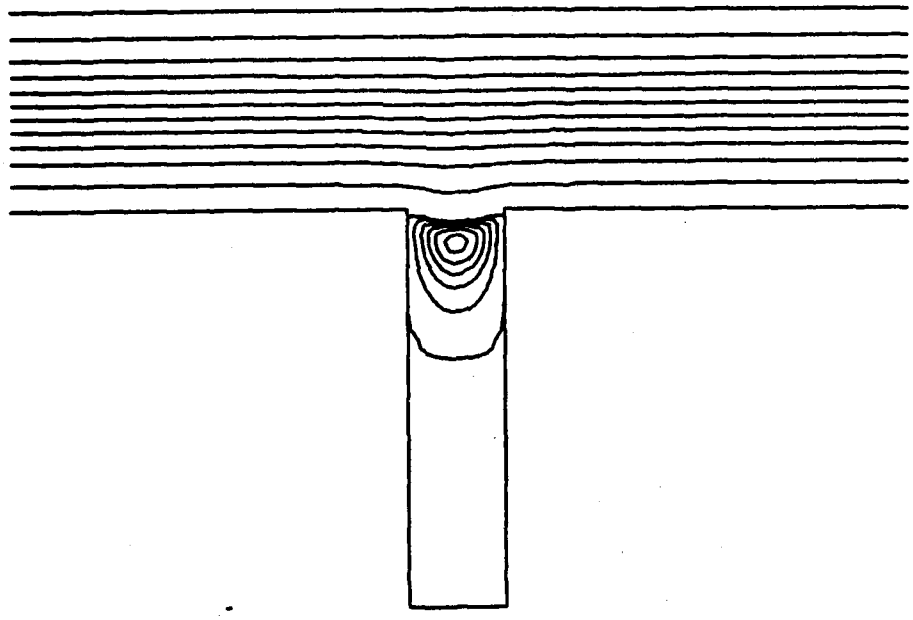

Figure 4

Stokes-flow in the Domain of Figure 2, Using the Mesh of Figure 3.

We note that the symmmetry of the streamlines is perfect to numerical accuracy, and any very slight deviations from symmetry in Figure 4 arise from the streamline integration used for graphical purposes [25]. This integration does not make use of the element-wise conic sections on triangles, but an approximate method. In all streamline plots shown here, the streamlines are not equally spaced contours throughout because the vortex in the slot is so faint in comparison to the flow outside. Instead, there are ten equally spaced contours outside the slot, the streamline at the wall in which the slot is cut, and five equally spaced contours in the slot. These latter contours have values which evenly divide the range of values between the streamline at the wall and the maximum value of the stream function.

We turn our attention to the non-Newtonian flow illustrated in Figure 5. Among other things, Figure 5 illustrates the fact that there are some constitutive equations with which rather high shear-rates can be obtained. Two non-dimensional numbers are useful in quantifying the degree of nonlinearity due to non-Newtonian effects,

$$\begin{aligned} D_e &\equiv \dot{\gamma}(T - \Lambda) \\ L_o &\equiv N_1/\sigma \end{aligned} \tag{21}$$

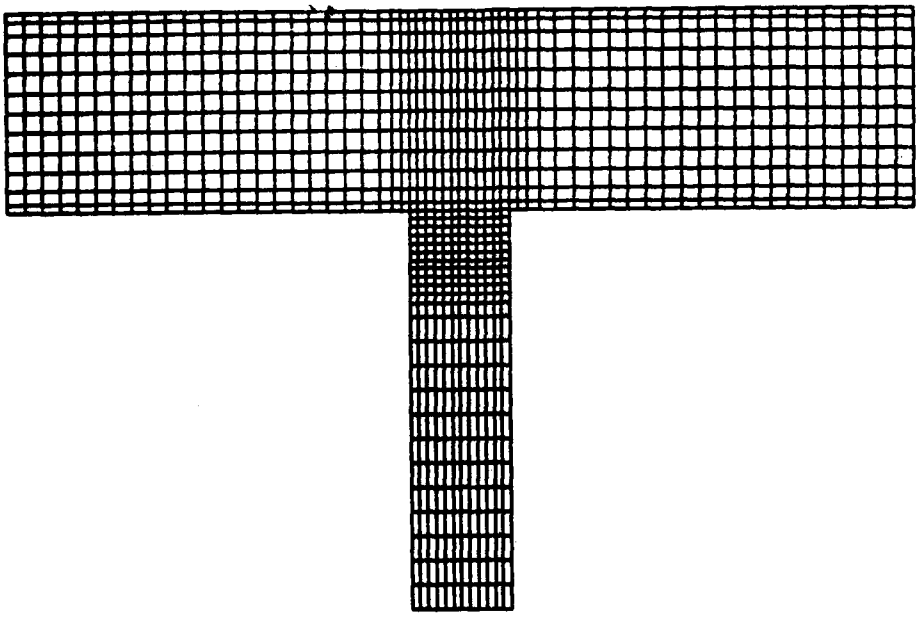

Figure 3

Mesh Discretizing the Domain of Figure 2 with 1008 Macroelements.

The distribution of elements was determined from extensive numerical experimentation, and the author believes it produces more accurate results than do any of those of ref. 10. The domain parameters of Figure 2 are $h = 1$, $b = 0.5$, and $q = 2$. Figure 4 shows a plot of the streamlines in Stokes-flow (Newtonian, zero Reynolds number) obtained using this mesh; this will serve as a useful baseline in what follows.

a long history and is discussed in some detail in refs. 3.4.10,17,20, and 22-25. It is of practical importance, because it seems feasible to design measurement devices based on the relation between P_e and N_1, which predict the latter based on continuous measurement of the former and the wall shear-stress in undisturbed flow, σ [10,23,24]. It has been found experimentally that the $P_e - N_1$ relation accurately describes the behavior of various viscoelastic fluids in flows over slots [23,24]. This appears to happen in spite of the fact that the assumptions behind the derivation [22] of eq. (20) are violated [10,23]. The purpose of the investigation undertaken by the author is to explore this apparent anomoly in detail, using his numerical techniques. Significant progress has been made in these investigations since the appearence of ref. 10; however, these results are best presented in a future publication. Here we will focus on some interesting qualitative features of plane flow over a transverse slot and the apparent relation of these qualitative features to the numerically observed hole-pressure. The results will also illustrate the dramatic and somewhat puzzling differences resulting from using different constitutive equations to study the same flow.

Numerical Results

Figure 3 illustrates a mesh of 1008 crossed-triangle macroelements, which has been designed by the author to discretize the domain of Figure 2 and to investigate hole-pressure problem of the previous subsection.

from which one may deduce that if $\mathbf{H}_k$ were the inverse Jacobian, eqs. (18) would be Newton's method. The inverse Broyden method given by eqs. (18) is a fairly robust method for computations with some constitutive equations, but it diverges at rather low Deborah numbers with others. The reason for this is not entirely clear at this point, but one avenue worth exploring fully is the possibility of finding more accurate approximations to the actual inverse Jacobian, and the author is currently involved in studying this matter.

A MODEL PROBLEM

Plane Flow over a Transverse Slot

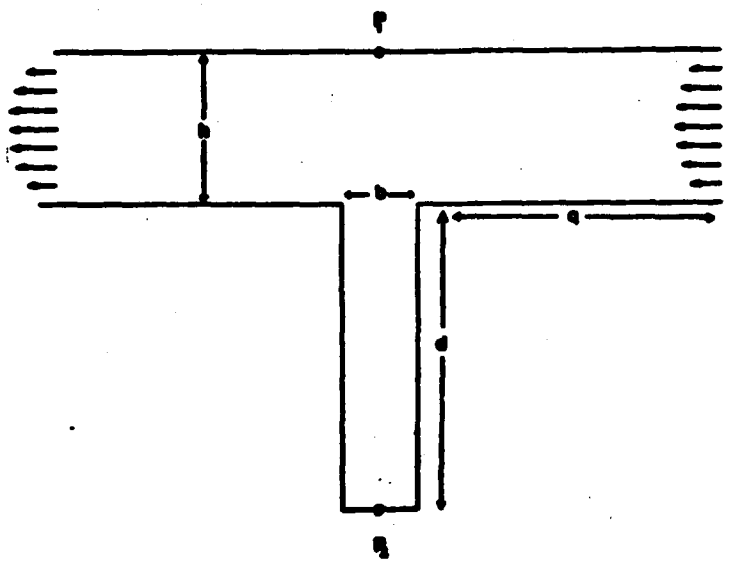

Figure 2

Domain for Plane Flow over a Transverse Slot.

Here we consider the flow of a viscoelastic fluid over a transverse slot [3,4,10,17,20,22-25]. The author [10,26] has been investigating the prediction that at negligible Reynolds number (based on slot width), the difference between the thrust on the wall at the top and bottom of the slot, pictured in Figure 2

$$P_e = P_1 - P_2 \tag{20}$$

is related to the first normal stress difference, N_1, in a simple fashion. This problem has

Solving the Nonlinear Equations

Here we briefly discuss the kind of numerical method which can be used to find the zero(s) of eq. (14). One may deduce that the functional dependence of the right-hand side of eq. (14) on the unknown velocity field is so complicated that Newton's method is difficult at best. On the other hand, it has been found that iterative methods based on the finite element approximation to the Stokes operator, which puts all nonlinearity on the right-hand side, do not have very favorable convergence properties, even at moderate Deborah numbers [2,7,19]. The method illustrated here is a Gauss-Newton type which begins from an estimate of the solution, $\mathbf{u_0}$, which represents nodal values of a finite element solution computed using the Stokes operator, but with inflow and outflow boundary conditions appropriate to the non-Newtonian solution (the "pseudo-Newtonian" solution). The iteration matrix is an approximation to the unavailable inverse Jacobian. The inverse Jacobian approximation begins using the Stokes approximation and continues, using rank-one updates, $\mathbf{r_i}$ and $\mathbf{v_i}$, to better approximate the inverse Jacobian as the iteration progresses. This method is known as the "inverse Broyden" method, and it is quite efficient, as it only requires a single matrix elimination proceedure to be carried out on $\mathbf{H_0}$.

$$
\begin{aligned}
&\textit{for } k = 0 \\
&\quad \mathbf{H_0} = \text{inverse Stokes' matrix}, \\
&\quad \mathbf{u_0} = \text{pseudo-Newtonian solution}, \\
&\quad \mathbf{R(u_0)} = \text{residual of eq. (15) at } \mathbf{u_0} \\
&\quad \mathbf{s_0} = -\mathbf{H_0 R(u_0)}
\end{aligned}
\tag{17}
$$

$$
\begin{aligned}
&\textit{for } k = 0, 1, 2, \ldots \\
&\quad \mathbf{u_{k+1}} = \mathbf{u_k} + \mathbf{s_k}, \\
&\quad \mathbf{y_k} = \mathbf{R(u_{k+1})} - \mathbf{R(u_k)}, \\
&\quad \mathbf{v_k} = \mathbf{H_k}^T \mathbf{s_k} / (\mathbf{s_k}^T \mathbf{H_k y_k}), \\
&\quad \mathbf{r_k} = \mathbf{s_k} - \mathbf{H_k y_k}, \\
&\quad \mathbf{H_{k+1}} = \mathbf{H_0} + \textstyle\sum_{i=0}^{k} \mathbf{r_i v_i}^T, \\
&\quad \mathbf{s_{k+1}} = [1 - \mathbf{v_k}^T \mathbf{R(u_{k+1})}] \mathbf{r_k}, \\
&\textit{next } k.
\end{aligned}
\tag{18}
$$

By rearrangement of eq. (18), it follows that

$$
\begin{aligned}
\mathbf{u_{k+1}} - \mathbf{u_k} &= \mathbf{s_k} \\
\mathbf{s_k} &= \mathbf{H_k R(u_k)},
\end{aligned}
\tag{19}
$$

The Stream and Drift Functions

The construction of the particle paths of Figure 1 and the accumulation of the deformation-gradient via eq. (13) are the dominant computational cost of the method presented here. There are several interesting aspects of the chosen finite elements which contribute to the efficiency with which this can be done. Since the interpolating functions determining the test and trial functions on each triangle are linear, it follows that there is a quadratic stream function on each triangle, $\psi(\mathbf{x})$ (it actually turns out to be a quadratic spline on the whole mesh). Thus the boundary crossings illustrated in Figure 1 can be found in sequential triangles upstream of each $\boldsymbol{\xi}_e$ using the quadratic formula,

$$\begin{aligned} \psi(\mathbf{x_1}) &= \psi(\mathbf{x_2}) \\ l(x_2^1, x_2^2) &= 0 \end{aligned} \tag{15}$$

The relation involving $l(\cdot,\cdot)$ is the requirement that $\mathbf{x_2}$ be on the line defining one of the boundaries of the current triangle. Thus eq. (15) is a quadratic equation in one of the components of $\mathbf{x_2}$, either x_2^1 or x_2^2. To associate a historical time with $\mathbf{x_2}$, it turns out that for the chosen elements, the time of transit between two points on the same streamline can be determined from the *drift function*, which is known analytically [10].

$$\tau_1 - \tau_2 = w(\mathbf{x_1}) - w(\mathbf{x_2}) \tag{16}$$

The drift function is denoted by w; its analytic expression involves various cases depending on the characteristics of the pathline equations in eq. (7) [10]. Stress calculation can thus proceed by finding boundary crossing points only and accumulating strain at these points via eq. (13), using the times associated with the boundary crossings computed via eq. (16). The accumulation proceeds until the boundary crossing times in one element, τ_1 and τ_2, bracket one or more temporal integration points of eq. (11), at which time(s) the integrand of eq. (11) can be evaluated using the analytic expression for the strain [10] and eq. (13) with τ taken as the value of the temporal integration point(s). Since there are potentially six solutions to eqs. (15), when each boundary of the current triangle is considered as a possible candidate on which to find $\mathbf{x_2}$, the drift function is also indispensible in determining the actual boundary crossing of a particle as the one which gives the maximum value of τ_2 satisfying $\tau_2 < \tau_1$.

by

$$\mathbf{E}_0(\tau) = \mathbf{E}_0(\tau_1)\mathbf{E}_{\tau_1}(\tau) \tag{13}$$

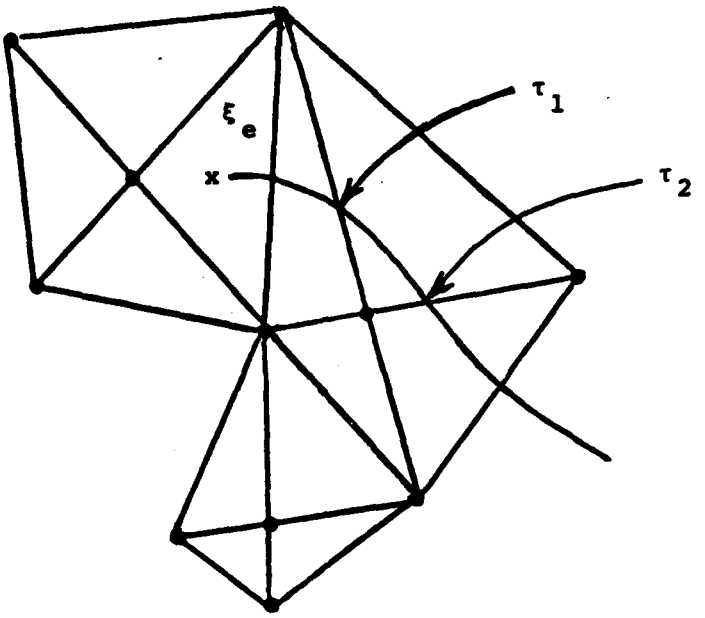

Figure 1
Composite Elements and Particle Paths for Right-Wing Method.

The computation of stress may thus proceed by piecing together streamlines and strain-measures along them analytically. This process is illustrated in Figure 1. Inspection of the discrete Galerkin equation

$$\sum_e \theta_e[\boldsymbol{\sigma}' \cdot \nabla \mathbf{v}^h + 2z(\nabla \cdot \mathbf{u}^h)(\nabla \cdot \mathbf{v}^h) + \rho(\mathbf{u} \cdot \nabla)\mathbf{u}^h \cdot \mathbf{v}^h - \mathbf{v}^h \cdot \mathbf{F}](\xi_e) = 0 \tag{14}$$

shows that, with the computation of stress at a finite number of favored points in the domain, an approximation to the Galerkin residual of the equations of motion can be obtained. Eq. (14) comes from numerically integrating the usual Galerkin residual of the equations of motion (8); θ_e is the area of triangle e in the finite element mesh, ξ_e is the corresponding triangle centroid (spatial integration point). $\mathbf{v}^h$ is an arbitrary Galerkin test function, expanded in the same type of interpolations in which the desired discrete solution, $\mathbf{u}^h$, is expanded. The parameter, z, is the penalty parameter, which allows nearly exact satisfaction of the continuity equation (9) implicitly in the Galerkin formulation [10].

at discrete points in historical time, τ_k. For a single relaxation time, or $N = 1$ in eq. (5), the Gaussian formula is given by the well-known Laguerre family of formulas. For other memory functions (assumed to be sums of exponentials here), analogous formulas can be derived [10]. It should be pointed out that the number, N_p, of integration points is not explicitly related to the number, N, of relaxation times (which is often infinite). This is in distinct contrast to the situation with differential constitutive equations, where each relaxation time adds a new partial stress and a new set of stress equations to be solved. With the integral form, adding relaxation times need not increase N_p and the corresponding computational effort. Experience shows, however, that if adding relaxation times significantly spreads out the relaxation spectrum, an increased N_p may be required to maintain accuracy.

Evaluating the Strain

The author has chosen a basic approach to solving the tracking equations (7) which involves the choice of finite elements for which the solution for the particle pathline (streamline) is known exactly in piecewise fashion as it crosses each element. For this purpose, the quadrilateral element composed of four linear triangles defining the diagonals of the quadrilateral have been chosen; these are illustrated in Figure 1. The composite pattern is chosen to produce accurate satisfaction of the continuity equation with an element of sufficient over-all accuracy. Linear triangles in other arrangements will not do this. In order to compute the integrand of eq. (11), we observe that if a pathline is known, the strain measures of eq. (6) are readily computed from nodal variables and assumed interpolations if $\mathbf{E_0}(\tau)$ is known. $\mathbf{E_0}$ is the solution to the evolution equations for the deformation-gradient, which are part of eqs. (7). This solution is known piecewise analytically on each element of the type which is employed. We proceed as follows: We define $\mathbf{E_0}(\tau_1)$ to be the solution to the strain evolution equations back to historical time τ_1, at which the particle being tracked is located at the boundary of some triangle in the mesh. We define $\mathbf{E}_{\tau_1}(\tau)$ to be the solution to the following strain evolution equation, which is derived from eq. (7) by modifying the initial condition to an interface condition:

$$\begin{aligned} \dot{\mathbf{E}}_{\tau_1} &= \mathbf{F}\mathbf{E}_{\tau_1} \\ \mathbf{E}_{\tau_1}(\tau_1) &= \mathbf{I} \end{aligned} \tag{12}$$

It turns out that $\mathbf{E}_{\tau_1}$ can be easily determined analytically for the chosen elements [10]. The whole deformation-gradient back to $\tau < \tau_1$ can then be mutiplicatively accumulated

fundamental difference between integral and differential forms is only the question as to whether a closed-form quadrature is known for the stresses or integration of ODEs along the streamlines is required.

An alternative way to look at Table 1 is as an indicator of the degree of "Lagrangianess" of the various methods. From that point of view, the left and right wings of the table do not define extremes any longer. One may properly consider the left-wing methods to be totally Eulerian in that all quantities solved for are referred to fixed spatial locations and not to particles. as we move rightward on the table, streamlines — and thus particle paths — begin to play an increasingly important role. But the right-wing methods still retain the equations of motion in Eulerian form and are only partially Lagrangian in their need to track particles in order to compute stresses. At the far right wing of Lagrangianess is found Hassager's method [21], which uses a deforming mesh. This method has some drawbacks — particularly in flows with recirculations — but the method is worthy of note because it seems to be the only method currently employed which can do transient analysis with integral constitutive equations.

COMPUTATION WITH A SINGLE-INTEGRAL MODEL

It seems appropriate to present some numerical results in this paper, but in so doing we must of necessity limit our consideration to those results with which the author is most familiar. This means that we will look at the extreme right-wing method of Table 1, applied to a flow which is essentially a measurement flow. We first turn our attention to an overview of some of the problems associated with the implementation of a particle-tracking, pure $\mathbf{v}, p$ method. More details may be found in refs. 7 and 10.

Evaluating the History-Integral

The most basic problem to be dealt with in devising a numerical method for integral constitutive equations is the numerical approximation of the history-integrals in the stress calculator, eq. (4). Consider a typical memory function, $m(\tau)$; the most efficient way to compute the history-integral, presuming the components of the strain measure are known, is via a Gaussian formula,

$$\int_{-\infty}^{0} \mathbf{S}_0(\tau) m(\tau)\, d\tau \approx \sum_{k=1}^{N_p} \omega_k \mathbf{S}_0(\tau_k) \tag{11}$$

The formula is in the form of a weighted sum with weights, ω_k, of the integrand evaluated

The middle-of-the-road methods in Table 1, at first sight, seem applicable only to differential models and thus seem to be left-wingers at heart, but on closer examination, they point the way to a unification of the two extremes. The middle-of-the-road methods are currently under development by Tanner and coworkers [18], and Variant 2 currently exists only as a boundary-integral method, but its obvious extension to a finite element method make it appropriate to this discussion. Both Variants 1 and 2 begin with an estimated velocity field and soive alternate hyperbolic and elliptic problems for stress and velocity, using ideas related to the obsevation of eqs. (10a). Variant 1 uses a discrete hyperbolic method to solve for the stress, and Variant 2 uses the fact that, in the current velocity iterate, the streamlines are characteristics, and thus the stress equations can be reduced to ordinary differential equations along them. These methods do not alleviate the drawbacks of the extreme methods, but rather represent a different balance of trade-offs. They require separate extra stress calculation, but fewer unkowns in each phase than the left-wing methods. Each added extra stress requires an extra pass through the stress-equation solver, not more simultaneously active unknowns. The middle-of-the-road methods require hyperbolic data, but Newton's method and transient analysis do not seem as forbidding as with right-wing methods.

However, the most important aspect of the middle-of-the-road methods is the bridge between the extreme methods they illuminate. Combination of Variant 2 and the analytic streamline version of the right-wing method seem to show real promise of allowing the development of a "supermethod," applicable to either differential or integral models, which shares as much code as possible in the computations with either kind of constitutive equation. The common portion of the code constructs the mesh and guides the nonlinear iterations (among other functions) and constructs streamlines by the procedures already in place in the analytic streamline version of the right-wing methods. Depending on whether the constitutive equation is integral or differential, a stress-integral evaluator or a stress ODE integrator is plugged in to evaluate the stress along the streamlines. The supermethod will take some time to develop, since solving hyperbolic equations numerically is not a trivial task. For example, one can forsee some difficulty associated with the specification of initial/end conditions for the stress ODEs on the streamlines. For incoming streamlines, stress can probably can be specified as data, but on closed streamlines, periodic end-conditions seem appropriate. How to do this without excessive "shooting" is not clear at present. But the possibility of the existence of a supermethod points out that the

slot than they are in Stokes-flow. Careful comparison of Figures 4, 6, and 7 show that the streamline nearest the slot is in virtually the same position in both Stokes-flow and the non-Newtonian flow, but that in both Figures 6 and 7, the streamline dips measureably futher down. Also, in distinct contrast to the flow of Figure 5, numerical results reported elsewhere [4,10], and flow visualizations [4], the vortices in Figures 6 and 7 are higher up and nearer the slot mouth than they are in Stokes-flow. It seems that with the concocted constitutive equation, the flow in the slot interacts with and disturbs the channel-flow to a much greater extent than it does in the Curtiss-Bird case.

It would be easy to dismiss the differences between the two constitutive equations discussed here as an unphysical consequence of the artificially concocted constitutive equation; however, behavior like that observed with the concocted equation seems to be characteristic of *all* the integral constitutive equations the author has tested, *except* the Curtiss-Bird. And the behavior seems to be worse for other equations; the tinkering applied to the Johnson-Segalman model has produced the second best constitutive equation to the Cirtiss-Bird, measured by the ability to get to high D_e and/or L_o. The difference between the two constitutive equations seems to devolve from the amount of shear-thinning at a given elasticity; this can be quantified by observing L_o as a function of σ in simple shear. The Curtiss-Bird equation leads to an L_o vs. σ curve with positive curvature, while the concocted equation has negative curvature. This leads to a prediction [22], which is observed numerically, that P_e/N_1 should be larger at fixed σ for the concocted equation than it is for Curtiss-Bird. Referring to Figures 5 and 7, we can see that the component of cross-stream normal force acting along the streamline should be less for the Curtiss-Bird fluid than it is for the concocted equation, since in the Curtiss-Bird case, the streamlines are much more nearly parallel to the wall. Thus we are brought back to the old arguement of Tanner and Pipkin [26], in which the non-zero values of P_e observed experimentally are attributed to elastic restoring forces acting on a control volume over the slot. This kind of explanation of viscoelastic hole-pressure seems to be borne out in these numerical results, at least on a qualitative level. It is also interesting to observe that the same interaction between slot and channel-flow which causes relatively higher hole-pressure seems to cause numerical difficulty. It is tempting to speculate that the numerical difficulty may be due to an impending breakdown of steady channel-flow near the slot mouth, due to this interaction.

CONCLUSIONS

The author believes that the numerical methods decribed here represent an auspicious beginning to the task of numerically modelling non-Newtonian flows; however, they represent only a beginning. There needs to be a better theoretical understanding of the nature of the equations and the resulting approximation schemes before definitive progress can be made. Recent work illuminating the nature of the characteristics of the equations moves in that direction and serves to illustrate common ground between the different classes of constitutive theories proposed by rheologists. It is hoped that this can lead to a more unified numerical approach to this challenging and demanding class of problems. In the meantime, current numerical techniques, though only partially understood, seem to be capable of uncovering physically important consequences of non-Newtonian fluid behavior.

Acknowledgements: The numerical techniques for integral constitutive equations described here were developed jointly by the author and B. Bernstein (Dept. Mathematics, I. I. T.).

REFERENCES

1. R. I. TANNER, R. E. NICKEL, and R. W. BILGER, Finite element methods for the solution of some incompressible non-Newtonian fluid mechanics problems with free surfaces, *Comp. Meth. Appl. Mech. Eng. 16*, 155 (1975).
2. H. COURT, K. WALTERS, and R. DAVIES, Long-range memory effects in flows involving abrupt changes in geometry. Part 4: Numerical simulation using integral rheological models, *J. Non-Newtonian Fluid Mechs. 8*, 95 (1981).
3. G. D. RICHARDS and P. TOWNSEND, A finite element computer model of model of the hole-pressure problem, *Rheologica Acta 20*, 261 (1981).
4. T. COCHRANE, K. WALTERS, and M. F. WEBSTER, On Newtonian and non-Newtonian flow in complex geometries, *Phil. Trans. Roy. Soc. London, 301*, 163 (1982).
5. K. WALTERS, "Rheometry," Chapman and Hall, London (1975).
6. R. I. TANNER, Constitutive equations for the computing person, This volume (1985).
7. M. J. CROCHET, A. R. DAVIES, and K. WALTERS, "Numerical Simulation of Non-Newtonian Flow," Elsevier, Amsterdam (1984).
8. C. J. S. PETRIE, "Elongational Flows," Pittman, London (1979).
9. C. J. S. PETRIE, Measures of deformation and convected derivatives, *J. Non-Newtonian Fluid Mechs. 5*, 53 (1975).
10. D. S. MALKUS and B. BERNSTEIN, Flow of a Curtiss-Bird fluid over a transverse slot using the finite element drift-function method, *J. Non-Newtonian Fluid Mechs. 16*, 77(1984).
11. D. D. JOSEPH, M. RENARDY, and J. C. SAUT, Hyperbolicity and change of type in the flow of viscoelastic fluids, *Arch. Rat. Mech. Anal.*, to appear.
12. M. W. JOHNSON and D. SEGALMAN, A model for viscoelastic fluid behavior which allows non-affine deformation, *J. Non-Newtonian Fluid Mechs. 2*, 255 (1977).
13. M. DOI and S. F. EDWARDS, Dynamics of concentrated polymer systems. Parts I-IV, *J. C. S. Faraday 74 and 75*, 1789 (1978), 1802 (1978), 1818 (1978), 38 (1979).
14. C. F. CURTISS and R. B. BIRD, Kinetic theory for polymer melts. Parts I and II, *J. Chem. Phys. 74*, 2016 (1981).
15. M. CROCHET and R. KEUNINGS, Die swell of a Maxwell fluid: Numerical prediction, *J. Non-Newtonian Fluid Mechs. 7*, 199 (1980).

16. M. A. MENDELSON, P.-W. YEH, R. A. BROWN, and R. C. ARMSTRONG, Approximation error in finite element calculation of viscoelastic fluid flows, *J. Non-Newtonian Fluid Mechs. 10*, 31 (1982).
17. N. R. JACKSON and B. FINLAYSON, Calculation of hole pressure: II Viscoelastic fluids, *J. Non-Newtonian Fluid Mechs. 10*, 71 (1982).
18. M. B. BUSH, R. I. TANNER, and N. PHAN-TIEN, A boundary element investigation of extrudate swell, *J. Non-Newtonian Fluid Mech.*, to appear.
19. M. VIRIYAYUTHAKORN and B. CASWELL, Finite element simulation of viscoelastic flows, *J. Non-Newtonian Fluid Mechs. 8*, 245 (1981).
20. S. DUPONT, J. M. MARCHAL, and M. CROCHET, Finite element simulation of viscoelastic fluids of the integral type, Preprint, 1984.
21. O. HASSAGER and C. BISGAARD, A Lagrangian finite element method for the simulation of non-Newtonian liquids, *J. Non-Newtonian Fluid Mech. 12*, 155 (1983).
22. K. HIGASHITANI and W. G. PRITCHARD, A kinematic calculation of intrinsic errors in measurements made with holes, *Trans. Soc. Rheology 16*, 687 (1972).
23. A. S. LODGE and L. de VARGAS, Positive hole-pressures and negative exit pressure generated by molten low-density polyethelyne flowing through a slit die, *Rheologica Acta 22*, 151 (1983).
24. R. D. PIKE and D. G. BAIRD, Evaluation of the Higashitani and Pritchard analysis of the hole pressure using flow birefringence, *J. Non-Newtonian Fluid Mech. 16*, 211 (1984).
25. D. S. MALKUS, Finite element simulation of flows with integral constitutive equations, *Comm. Appl. Num. Meths.*, to appear.
26. R. I. TANNER and A. C. PIPKIN, *Trans. Soc. Rheol. 13*, 471 (1969).

SECURITY CLASSIFICATION OF THIS PAGE (When Data Entered)

REPORT DOCUMENTATION PAGE	READ INSTRUCTIONS BEFORE COMPLETING FORM
1. REPORT NUMBER: 2812	2. GOVT ACCESSION NO.: AD-A154 877
	3. RECIPIENT'S CATALOG NUMBER:
4. TITLE (and Subtitle): FINITE ELEMENT METHODS FOR VISCOELASTIC FLOW	5. TYPE OF REPORT & PERIOD COVERED: Summary Report - no specific reporting period
	6. PERFORMING ORG. REPORT NUMBER:
7. AUTHOR(s): David S. Malkus	8. CONTRACT OR GRANT NUMBER(s): DAAG29-80-C-0041, 84-NM-399, MCS 79-03542, 81-02089 and 83-01433
9. PERFORMING ORGANIZATION NAME AND ADDRESS: Mathematics Research Center, University of Wisconsin, 610 Walnut Street, Madison, Wisconsin 53706	10. PROGRAM ELEMENT, PROJECT, TASK AREA & WORK UNIT NUMBERS: Work Unit #2 & #3 (Physical Mathematics, Numer. Analysis and Scientific Computing
11. CONTROLLING OFFICE NAME AND ADDRESS: (See Item 18 below)	12. REPORT DATE: April 1985
	13. NUMBER OF PAGES: 28
14. MONITORING AGENCY NAME & ADDRESS (if different from Controlling Office)	15. SECURITY CLASS. (of this report): UNCLASSIFIED
	15a. DECLASSIFICATION/DOWNGRADING SCHEDULE

16. DISTRIBUTION STATEMENT (of this Report)

Approved for public release; distribution unlimited.

17. DISTRIBUTION STATEMENT (of the abstract entered in Block 20, if different from Report)

18. SUPPLEMENTARY NOTES

U. S. Army Research Office, P. O. Box 12211, Research Triangle Park, North Carolina 27709

Air Force Office of Scientific Research, Washington, DC 20332

National Science Foundation, Washington, DC 20550

19. KEY WORDS (Continue on reverse side if necessary and identify by block number)

constitutive equation, viscoelastic fluid, finite element, measurement flow, differential model, integral model, characteristics, streamlines, hole-pressure

20. ABSTRACT (Continue on reverse side if necessary and identify by block number)

Finite element methods to compute approximate solutions to flow problems involving the flows of viscoelastic fluids are discussed. The primary goals of such investigations are at least three: First, to evaluate the predictions of the many proposed constitutive theories for viscoelastic fluids. Second, to model measurement flows in various rheological measurement devices in order to quantify the deviation of the actual flow from the flow which must be presumed to interpret the measurement. Third, it is hoped that these methods will prove sufficiently robust to allow the simulation of idealized polymer processes with

(cont.)

DD FORM 1 JAN 73 1473 EDITION OF 1 NOV 65 IS OBSOLETE

UNCLASSIFIED

SECURITY CLASSIFICATION OF THIS PAGE (When Data Entered)

ABSTRACT (cont.)

the aim of aiding in the design of such processes and the required apparatus. The focus of the current research of the author and a growing number of others is on two-dimensional, isothermal, steady flows of incompressible fluids. While these restrictions will be seen to be nonessential in theory, even the simplest calculations of non-viscometric flow solutions will be seen to require a high degree of computational complexity in practice. Nevertheless, the current finite element procedures seem to show promise in the continuing endeavor to understand this challenging class of problems.

END

FILMED

7-85

DTIC